Strength and drying shrinkage of slag paste activated by sodium carbonate and reactive MgO

Fei Jin*, Abir Al-Tabbaa

Fei Jin: PhD candidate, Department of Engineering, University of Cambridge, Trumpington Road, Cambridge CB2 1PZ, United Kingdom

Abir Al-Tabbaa: PhD, Reader in Department of Engineering, University of Cambridge, Trumpington Road, Cambridge CB2 1PZ, United Kingdom

* Corresponding author

Email: leonking1987@gmail.com

Abstract: This paper investigates the potential of combining Na_2CO_3 and reactive MgO as a sustainable activator for ground granulated blastfurnace slag. Two very different reactivity MgOs were added at 5-10 % and the Na_2CO_3 content varied from 4% to 8% by the weight of slag. The strength and the drying shrinkage of the activated slag pastes were tested up to 90 days. It was found that the optimum reactive MgO addition was 5% regardless of the MgO type and Na_2CO_3 content. MgO with the higher reactivity significantly increased the early strength of the paste but had almost no effect on the strength at 90 days. On the other hand, the effect of the lower reactivity MgO on the strength was more profound at later ages and low Na_2CO_3 dosage. In terms of drying shrinkage, increasing the Na_2CO_3 content from 4% to 6% caused a remarkable decrease of drying shrinkage while increasing it from 6% to 8% had negligible effect. X-ray diffraction and thermogravimetric analysis revealed that the major hydration products were calcium silicate hydrate gel and hydrotalcite-like phases, similar to those in conventional alkali-activated slags. There was also a large quantity of calcite formed especially in the 8% Na_2CO_3 pastes due to causticisation. It was concluded that the combination of reactive MgO and Na_2CO_3 could serve as a potential sustainable activator for slags.

Keywords: reactive MgO, sodium carbonate, slag, strength, drying shrinkage, hydration products

1. Introduction

The production of Portland cement (PC) results in ~7% of man-made CO_2 emissions [1], from the decomposition of limestone at ~1450 °C, the combustion of fuels in the kiln, as well as from power generation. Various attempts have been made in order to reduce the carbon footprint of the cement industry, one of which is the extensive usage of industrial by-products. Alkali-activated slag cements (AAS) based on ground granulated blast-furnace slag (GGBS) are sustainable alternatives to PC due to their low initial capital cost of the raw material, the saving of energy and resources, and the elimination of CO_2 emissions from limestone decomposition [2]. It is estimated that 70-80% of the CO_2 emissions can be reduced by substituting alkali-activated binders for PC [3].

Numerous research efforts have focussed on the activation of GGBS by various alkali-metal hydroxides and silicates such as NaOH, KOH, sodium silicate and their mixtures [4]. However, neither NaOH nor sodium silicate is naturally available and they both require energy-intensive manufacturing processes. NaOH is usually generated by electrolysis of sodium chloride solution while sodium silicate is mainly produced by melting sand together with sodium carbonate/sodium sulfate at 1100-1200 °C followed by dissolution at 140-160 °C in high pressure steam. Consequently, the production of these alkalis has a large carbon footprint which diminishes the environmental credits assigned to AAS. Therefore, AAS using high volumes of NaOH and sodium silicate cannot be regarded as the best option for achieving a truly low-carbon and environmentally friendly cement system [5]. In addition to these sustainability challenges, the caustic nature, high cost and significantly high drying shrinkage behaviour [6] hinder the widespread usage of AAS based on these activators.

To develop a more sustainable AAS cement, sodium carbonate (Na_2CO_3) was proposed as an alternative activator for GGBS [7]. Na_2CO_3 can be refined from the mineral trona, or from naturally occurring sodium-carbonate-bearing brines, or alternatively manufactured from one of several chemical processes, and thus the world's resources of Na_2CO_3 are practically inexhaustible and it is 2-3 times cheaper than NaOH or sodium silicate [8]. Furthermore, Na_2CO_3 is less caustic and less harmful to the environment since it only produces carbonate anions in water. Nevertheless, research

on Na_2CO_3 activated slag is still very limited in the literature. Fernandez-Jimenez [7] showed that at 28 d, the strengths of alkali activated slag mortars followed the order: Na_2SiO_3•nH_2O+NaOH > Na_2CO_3 > NaOH. The author and later studies [6,9] suggested that Na_2CO_3 activated slag pastes showed long setting times and low early strength due to the low initial pH and the formation of a sodium calcium carbonate which retarded the reaction process. At later ages, the strengths were higher in the case of Na_2CO_3 due to the formation of carbonated compounds such as C_3A•$CaCO_3$•$12H_2O$ [10]. Sakulich et al. [11] found that Na_2CO_3 (8% of slag) activated slag mortar had negligible strength at 1 d while the strength increased to ~37 MPa at 28 d, with ~75% of this strength gained during the first week. In terms of shrinkage, Andersson and Gram [12] revealed that although the drying shrinkage of 5% Na_2CO_3 activated slag was ~60% higher than PC at 231 d of curing at 20°C and 80% RH, curing at 80°C for 8 hours significantly decreased the shrinkage to a value slightly lower than that of PC. In another study, Duran Atis [6] found that the shrinkage of sodium silicate and NaOH activated slag mortar was 3 and 6 times more than that of PC mortar, respectively; while the shrinkage of Na_2CO_3 activated slag mortar was lower or similar to PC mortar at 23 °C and 65% RH. Therefore, Na_2CO_3 could be a promising sustainable activator to produce low-shrinkage AAS.

In fact, Na_2CO_3 is often used with other alkaline activators such as NaOH or sodium silicate. Collins and Sanjayan [13] evaluated the suitability of NaOH and Na_2CO_3 as a joint activator for slag and compared them with PC cured at 23 °C. With the addition of Na_2CO_3, the results indicated that the 1 d strength was generally greater than PC at the higher dosage levels of NaOH and Na_2CO_3, and there was a trend of increasing strength with increasing Na_2CO_3 dose. Similarly, Li and Sun [14] showed that the combination of NaOH and Na_2CO_3 gave higher strengths than using either alone. Fernandez and Puertas [9] investigated the combination of sodium silicate, NaOH and Na_2CO_3 and indicated that the silicate anions increased while the carbonate anions decreased the strength of the AAS pastes. Recently, Yang et al. [2] used the combination of $Ca(OH)_2$ and Na_2CO_3 to activate GGBS and found that the hydration products were calcium silicate hydrate (C-S-H) gel, gehlenite hydrate (C_2ASH_8),

calcium aluminium hydrate (C_4AH_{13}), and magnesium silicate hydrate (M-S-H) gel. In terms of strength, the combination of $Ca(OH)_2$ and Na_2CO_3 gave ~20% increase over that using $Ca(OH)_2$ alone.

Hard-burned MgO (calcined at ~1000-1200 °C) has been used as an expansive additive for PC-based concrete in large concrete dam construction in China for decades [15]. Reactive MgO is usually calcined at 700-1000 °C and has a higher reactivity than the hard-burned, as well as the dead-burned MgO produced ≥ 1400 °C, which is usually present in PC. However, the physical and chemical properties of reactive MgO vary considerably, which are primarily governed by the source of the precursor and calcination history [16]. Recently, reactive MgO was found to be an alternative activator for GGBS, and gave higher strengths than $Ca(OH)_2$ activated GGBS at > 28 d [17,18]. The effect of reactive MgO in the AAS systems has also been investigated. Shen et al. [19] showed that the addition of 10% reactive MgO reduced the shrinkage of sodium silicate activated slag/fly ash (AAFS) cement by ~50%, and the shrinkage was only slightly higher than that of PC. Meanwhile, the compressive strengths up to 7 d were found to increase slightly while the 28 d strength remained unchanged. Jin et al. [20] studied the strength and drying shrinkage of reactive MgO modified sodium silicate activated GGBS pastes using two different reactive MgO. They showed that MgO with high reactivity accelerated the early hydration of AAS and significantly decreased the drying shrinkage. Although MgO with medium reactivity had little effect on the early strength, it also decreased the drying shrinkage of AAS. Previous findings [18,20,21] showed that reactive MgO was mainly consumed by the reaction with GGBS to form hydrotalcite-like phases (M-A-H), which contributed to the strength gain and the shrinkage reduction.

This paper aims to investigate the suitability of combining reactive MgO and Na_2CO_3 for the activation of GGBS. The effect of two different reactive MgOs with very different reactivities on the performance of the reactive MgO and Na_2CO_3 activated GGBS pastes was investigated. The unconfined compressive strength and drying shrinkage of the pastes were measured at different curing ages. The hydration products and the microstructure were followed by X-ray diffraction (XRD), thermogravimetric analysis (TGA) and scanning electron microscopy (SEM).

2. Materials and Methods

The GGBS used in this study, with a hydraulic index of 1.6 according to [22], was obtained from Hanson, UK. Two different reactive MgOs (from Richard Baker Harrison, UK) with different characteristics were used as the additive. Based on the characterisation in [23], the first was MgO_H, categorised as a highly reactive MgO, which almost completed its hydration in one day, and the second was MgO_M, defined as MgO with medium reactivity, which continued to hydrate after one month. The chemical compositions of the GGBS and reactive MgOs are shown in Table 1. Na_2CO_3 solution was prepared the day before mixing by dissolving the sodium carbonate anhydrite powders (Fisher Scientific, technical grade) in a predetermined amount of deionised water.

The Na_2CO_3 dosage varied from 4 % to 8 % by weight of GGBS while reactive MgO content ranged from 5 to 10 % by weight of GGBS. The mix compositions of all the paste samples are listed in Table 2 where N, H and M refer to Na_2CO_3, MgO_H and MgO_M respectively, with the Na_2CO_3 and MgO content followed by each notation. The water to solid (including the slag, reactive MgO and Na_2CO_3) ratio was fixed at 0.32. The MgO_H was only added with 4% Na_2CO_3 due to its large surface area causing significant decrease of workability as well as its high price. The reactive MgO powder was first mixed with the slag for 3 minutes in a bench-top mixer to achieve homogeneity to which the Na_2CO_3 solution was then added. After mixing for another 3 min, the mix was cast into the cubic (40×40×40 mm) or prism (40×40×160 mm) moulds in two layers and hand-vibrated to eliminate the voids. The samples were then covered with cling film to avoid moisture loss. After 24 hours, the samples were demoulded carefully and the cubes were transferred into the water tank maintained at 21±2 °C, while the prisms were stored at the temperature of 21±2 °C and relative humidity of 50±5%.

The drying shrinkage measurement was performed using a CONTROLS electronic length comparator with an accuracy of ±0.001 mm to determine the linear dimension variation of the prism specimen along the longitudinal axis. The first reading was recorded immediately after demoulding and the measurement was conducted in triplicate for each mix up to 90 days. The unconfined compressive strength (UCS) of the cubic samples, in triplicate, was determined according to [24] at the curing age

of 1, 3, 7, 28 and 90 days. Then the crushed samples were ground and stored in acetone for 3 days to arrest the hydration and then vacuum dried for ≥3 days followed by oven drying at 60 °C before microstructural analysis. The samples were then further ground to pass through a 75 micron sieve prior to XRD tests and TGA. XRD was carried out on a Siemens D5000 X-ray diffractometer using a scanning range from 5 to 55 (2θ), with a scanning speed of 1s/step and resolution of 0.05°/step. TGA was conducted on duplicate samples on PerkinElmer STA6000 equipment from 40 to 800 °C with the increasing rate of 10 °C/min. The standard error between two samples was in general less than 5%, so the average values were reported. SEM was performed on the JEOL 820 machine.

3. Results and Discussion

3.1. Strength development

Fig. 1 shows the UCS development of all the pastes in which it is apparent that the strength at 1 d increased significantly by the addition of MgO_H. At 7 and 28 d, the UCS development was the same for MgO_H based AAS, with 5% MgO_H addition showing the highest strength. However, the strength gain almost stopped at 28 d and approximately the same strength (~45-50 MPa) was obtained for the reference mix and the modified mixes at 90 d (Fig.1a). On the other hand, the strength was almost negligible at 1 d with MgO_M addition regardless of the Na_2CO_3 content. After 90 d of water curing, 4% Na_2CO_3 with 5% MgO_M content showed the highest strength and the reached ~65 MPa, which was ~45% higher than the reference mix (Fig. 1b). Nevertheless, higher dosages of MgO_M slightly decreased the strength at 28 d. At 6% Na_2CO_3 content, it was found that the addition of MgO_M did not increase the strength too much in the early ages (≤3 d). At 7 and 28 d, 5-7.5% MgO_M addition slightly increased the strength while 10% MgO_M reduced the strength compared to the reference mix. At 90 d, the mix with 5% MgO_M showed significantly higher strength than the other mixes (Fig. 1c). At 8% Na_2CO_3 content, no benefit of adding reactive MgO was observed in terms of strength during the first 28 d of curing. In addition, when the content of MgO_M was ≥ 5%, the strength decreased by ~12% compared to sample N8 (without MgO) at 90 d (Fig. 1d). Therefore, it was concluded that 5% of reactive MgO was the optimum content and the effect was dependent on the MgO type and the content of Na_2CO_3. At 4% of Na_2CO_3 concentration, 5% of MgO_H could effectively increase the early

strength of Na_2CO_3 activated GGBS while the long term strength was not affected. On the other hand, 5% of MgO_M helped to increase the strength at later ages (90 d), but gave no benefits to the early strength. Increasing the Na_2CO_3 content obscured the effect of reactive MgO.

3.2. Drying shrinkage

Fig. 2 shows the drying shrinkage values up to 90 d for the 4% Na_2CO_3 activated GGBS pastes with the addition of 5% and 10% of two reactive MgOs. It was found that the shrinkage of the pastes containing MgO_M was close to the reference (N4) during the first week. Afterwards, the shrinkage of the paste with 5% MgO_M only increased slightly from 28 d to 90 d, showing a final shrinkage decreased by ~13% than the reference (N4). Meanwhile, 10% of MgO_M increased the shrinkage by ~10%. On the other hand, MgO_H was much more effective in reducing the shrinkage of the AAS paste especially at early ages. It was observed that the shrinkage of the paste with 5% MgO_H addition (N4H5) showed 3 times less shrinkage than the reference at 1 d and still exhibited 50% less at 7 d. Finally, ~17% decrease in shrinkage was achieved at 90 d. Increasing the content of MgO_H to 10% slightly increased the shrinkage, though it was still much lower than the reference showing ~10% less shrinkage than the reference at 90 d.

The effect of the content of Na_2CO_3 and MgO_M on the drying shrinkage is illustrated in Fig. 3. It was apparent that increasing the Na_2CO_3 content from 4% to 6% significantly decreased (~53%) the shrinkage of the pastes, while no difference was detected when it increased from 6% to 8%. The addition of 5% of MgO_M showed the lowest shrinkage regardless of the Na_2CO_3 content, which is consistent with the strength results that 5% is the optimum MgO content. It should be noted that although no strength benefit was observed by adding MgO_M at 8% Na_2CO_3 content (Fig. 1d), the drying shrinkage decreased by ~30% at 28 d.

3.3. XRD results

The XRD patterns of the reactive MgO and Na_2CO_3 activated GGBS pastes cured for 28 d are shown in Fig. 4. Comparing the effects of the two reactive MgOs, MgO_H reacted much faster with slag to

produce more hydrotalcite-like phases which was indicated by the increased strongest characteristic peak of Ht at 2θ of ~11.7° (Fig. 4a), which increased with the increase of MgO content. Much higher peak of MgO was identified in pastes containing MgO_M indicating higher content of unhydrated MgO (indicated by the higher peak at 2θ of 42.9°) due to its lower reactivity compared to the pastes with MgO_H. It should be noted that there was no brucite detected in all the pastes regardless of the MgO type and content (≤ 10 wt%), which agreed well with previous studies [20,21], although a minor content of brucite out of the XRD detection limit could exist. A small peak for Na_2CO_3 at 2θ of 35° was detected suggesting that both the activators were not fully consumed by GGBS at28 d. In addition, characteristic peak for calcium sodium carbonate hydrate at 2θ of 47.7° was found. Various peaks for calcite were denoted in the patterns, which could be due to the carbonation of portlandite or C-S-H gel during the sample preparation and curing stages. It could also come from the causticisation of Na_2CO_3 as suggested in [25]:

$$Na_2CO_3 + Ca(OH)_2 = 2\ NaOH + CaCO_3 \quad (1)$$

Consequently, as it can be seen from the XRD curves, the peaks for calcite increased with the increase of Na_2CO_3 concentration.

Increasing the Na_2CO_3 content was found to increase the intensities of all the hydration products as illustrated in Fig. 4b, which indicates the enhancement of the slag hydration degrees and consequently higher strength. In addition, gehlenite hydrate as the minor hydration product was also observed, agreeing with [2].

The role of calcite played in the pastes is in analogy with hydrotalcite-like phases. Previous studies [10,26] on the role of limestone in slag cement indicated that calcite powder could refine the pore structure and improve the early strength. Therefore, an optimum content of reactive MgO (5% in this study) existed when the quantities of hydrotalcite-like phases and calcite were sufficient to give the lowest porosity and highest strength while higher contents would result in excess voluminous phases (i.e., hydrotalcite-like phases and/or brucite) and hence micro-cracks in the matrix leading to reduced strength.

3.4. TGA results

The TG and first derivative of TG (DTG) curves of the pastes cured for 28 d are shown in Fig. 5. The DTG curves were divided into four ranges:

1. At temperature up to 250 °C, this mainly involves the dehydration of C-S-H. In addition, M-S-H gel could also form by the reaction between MgO and dissolved SiO_2, and loses its water between 80-200 °C.
2. The temperature range of 250-450 °C includes mainly the decomposition of hydrotalcite-like phases, since brucite was found to be totally consumed by the reaction with slag from the XRD analysis.
3. The small shoulder at around 450-500 °C was attributed to the dehydration of portlandite.
4. The temperature range between 500 °C and 800 °C is the decomposition range of various carbonate-containing phases including magnesium carbonate, calcium carbonate, calcium sodium carbonate, sodium carbonate, and hydrotalcite-like phases.

The first two major weight losses (Δm_1 and Δm_2) and the total weight loss (Δm_t) were calculated by combining the TG and DTG curves and the results are shown in Table 3. It is apparent that with the increase of reactive MgO content, the total weight loss (i.e., chemically bound water content, CBW) increased. The effect of MgO_H was much greater than the MgO_M, due to the larger quantities of the C-S-H and hydrotalcite-like phases formed (indicated by the increase of Δm_1 and Δm_2) and the higher density of water in hydrotalcite-like phases. It also showed that the quantities of C-S-H and hydrotalcite-like phases increased much more significantly in pastes with 4% Na_2CO_3 than those with 8% Na_2CO_3, which was consistent with the strength results that the addition of reactive MgO was more effective with lower concentration of Na_2CO_3. In addition, the content of the carbonates was significantly higher in the samples with 8% Na_2CO_3 as indicated by the weight loss at 500- 800 °C.

To elucidate the effect of different reactive MgOs, the relationship between CBW and UCS of the paste with two types of MgOs and 4% Na_2CO_3 was plotted in Fig. 6. For MgO_M, there was a good linear relationship between CBW (as well as the MgO_M content) and UCS at 3 d indicating that the

MgO with lower reactivity led to a slower increase of hydration products. These newly formed products caused a gradual pore filing and consequently increased the strength of the pastes. At 28 d, with the increase of CBW (and MgO_M content), UCS increased up to MgO_M content of 5% while it decreased notably when MgO_M content reached 10%, suggesting that although the hydration products increased, the strength decreased, which could be due to the deterioration of the pore structure by excess hydrotalcite-like phases or a minor content of brucite that cannot be detected in XRD [20]. On the other hand, when highly reactive MgO (MgO_H) was used, this over filling effect was manifested at 3 d and continued till 28 d since it resulted in a much faster increase of hydration degree and the content of hydration products.

3.5. Microstructure

Fig. 7 shows typical SEM images of selected pastes at 3 d of curing. The early hydration product was mainly reticulated C-S-H (see Fig. 7a inset) covering the slag particles for the N4 and N4M5 samples at 3 d (Fig. 7a and c), resembling these observed in sodium silicate activated GGBS at early ages [20]. When 5% of highly reactive MgO (N4H5) or more Na_2CO_3 (N8) was used, relatively dense C-S-H gel was formed and showed a much less porosity than the former two (Fig. 7b and d), which were consistent with their strength and TGA results. The gels have occupied the spaces that were initially filled with water and generated a more compact microstructure, which further led to increased strength and more chemically bound water as presented above. Small crumbles in the N8 sample could be assigned to the excessive Na_2CO_3 or the calcite formed as explained in XRD section. It was concluded that MgO_H accelerated the early age hydration of the slag while MgO_M had almost no effect. There could be two effects by the addition of highly reactive MgO: (i) the quick hydration of MgO_H resulting in much more hydration products that can fill the pores more effectively and (ii) the fast heat release during the dissolution process of MgO leading to higher dissolution rate of GGBS and also higher reaction rate among the cement components. At 28 d, all mixes formed dense microstructure consisting primarily of C-S-H gels (Figure 8**)** and the other hydration products probably had no distinctive morphology and intermixed with the gels, which made them hard to identify. It should be noted that small cracks were visible in N4H5 sample, which could explain why its strength stopped to

gain from 28 to 90 d. Although hydration was still progressing as indicated by the TGA results, the cracks formed initially would expand and reduce the strength.

4. Conclusions

The mechanical and drying shrinkage properties of reactive MgO and Na_2CO_3 activated GGBS pastes were investigated in order to evaluate the suitability of combining reactive MgO and Na_2CO_3 as a sustainable activator for GGBS. The following conclusions can be drawn based on the experimental results obtained above:

1. It was found that an optimum content of reactive MgO (i.e., 5% by weight of the slag) existed regardless of the MgO type and Na_2CO_3 content. The effect of reactive MgO was more significant with low Na_2CO_3 content (4%), while at 8% Na_2CO_3 content, even with the optimum reactive MgO addition, the strength was almost the same as the reference.
2. MgO with high reactivity (~10 s) increased the early strength of Na_2CO_3 activated GGBS significantly while MgO with medium reactivity (~100 s) had no observable effect. However, the long term strength of pastes using highly reactive MgO was the same as the reference, while the addition of MgO with medium reactivity helped to increase the 90-d strength by ~45%.
3. In terms of drying shrinkage, increasing the Na_2CO_3 content from 4% to 6% caused a remarkable decrease of drying shrinkage while increasing it from 6% to 8% had negligible effect. Adding 5% reactive MgO can effectively reduce the drying shrinkage of Na_2CO_3 activated GGBS pastes regardless of Na_2CO_3 content.
4. XRD and TGA revealed that the major hydration products are C-S-H gel and hydrotalcite-like phases, with gehlenite hydrate as the minor phase. Both the MgO and Na_2CO_3 were not fully consumed at 28 d. In addition, there was a large quantity of calcite formed especially in 8% Na_2CO_3 pastes probably due to causticisation.

The combination of reactive MgO and Na_2CO_3 could serve as a promising sustainable activator for slags compared to the conventional caustic alkali hydroxides or silicates. In addition, considering the

low-shrinkage of Na_2CO_3 activated slag [6] and the shrinkage-reducing effect of MgO [15], this combination could probably generate AAS concrete with low drying shrinkage, facilitating the spread of AAS concrete. However, further research is needed to study other performance of this kind of AAS such as the setting time, rheology, and durability.

Acknowledgement

The first author is grateful to Cambridge Trust and China Scholarship Council (CSC) for sponsoring his PhD studentship.

References

[1] Metz B, Davidson O, Coninck H de, Loos M, Meyer L. IPCC Special Report on Carbon dioxide Capture and Storage. 2005.

[2] Yang K-H, Cho A-R, Song J-K, Nam S-H. Hydration products and strength development of calcium hydroxide-based alkali-activated slag mortars. Constr Build Mater 2012;29:410–9.

[3] Duxson P, Provis JL, Lukey GC, van Deventer JSJ. The role of inorganic polymer technology in the development of "green concrete." Cem Concr Res 2007;37:1590–7.

[4] Song S, Sohn D, Jennings H. Hydration of alkali-activated ground granulated blast furnace slag. J Mater Sci 2000;35:249–57.

[5] Rashad AM, Bai Y, Basheer PAM, Milestone NB, Collier NC. Hydration and properties of sodium sulfate activated slag. Cem Concr Compos 2012.

[6] Duran Atiş C, Bilim C, Çelik Ö, Karahan O. Influence of activator on the strength and drying shrinkage of alkali-activated slag mortar. Constr Build Mater 2009;23:548–55.

[7] Fernández-Jiménez A. Alkali-activated slag mortars Mechanical strength behaviour. Cem Concr Res 1999;29:1313–21.

[8] Kostick DS. Soda Ash: Statistics and Information. U.S. Geological Survey. 2013.

[9] Fernández-Jiménez A, Puertas F. Effect of activator mix on the hydration and strength behaviour of alkali-activated slag cements. Adv Cem Res 2003;15:129–36.

[10] Wang SDS, Scrivener KLK, Pratt P. Factors affecting the strength of alkali-activated slag. Cem Concr Res 1994;24:1033–43.

[11] Sakulich AR, Anderson E, Schauer C, Barsoum MW. Mechanical and microstructural characterization of an alkali-activated slag/limestone fine aggregate concrete. Constr Build Mater 2009;23:2951–7.

[12] Andersson R, Gram HE. Properties of alkali-activated slag concrete. Nord Concr Res 1987;6:7–18.

[13] Collins F, Sanjayan JG. Early Age Strength and Workability of Slag Pastes Activated by NaOH and Na2CO3. Cem Concr Res 1998;28:655–64.

[14] Li Y, Sun Y. Preliminary study on combined-alkali–slag paste materials. Cem Concr Res 2000;30:963–6.

[15] Lou Z, Ye Q, Chen H, Wang Y, Shen J, Lou Z, et al. Hydration of MgO in clinker and its expansive property. J CHINESE Ceram Soc 1998;26:430–6.

[16] Shand MA. The Chemistry and Technology of Magnesia. Hoboken, New Jersey: John Wiley & Sons, Ltd.; 2006.

[17] Yi Y, Liska M, Al-Tabbaa A. Properties and microstructure of GGBS-MgO pastes. Adv Cem Res 2014; 26:114-22.

[18] Jin F, Gu K, Al-Tabbaa A. Strength and hydration properties of reactive MgO-activated ground granulated blastfurnace slag paste. Cem Concr Compos 2014 (Accepted).

[19] Shen W, Wang Y, Zhang T, Zhou M, Li J, Cui X. Magnesia modification of alkali-activated slag fly ash cement. J Wuhan Univ Technol Sci Ed 2011;26:121–5.

[20] Jin F, Gu K, Al-Tabbaa A. Strength and drying shrinkage of reactive MgO modified alkali-activated slag paste. Constr Build Mater 2014;51:395–404.

[21] Jin F, Gu K, Abdollahzadeh A, Al-Tabbaa A. Effect of different reactive MgOs on the hydration of MgO-activated ground granulated blastfurnace slag paste. J Mater Civ Eng 2013.

[22] Mantel DG. Investigation into the hydraulic activity of five granulated blast furnace slags with eight different Portland cements. ACI Mater J 1994;91.

[23] Jin F, Al-Tabbaa A. Characterisation of different commercial reactive magnesia. ICE Adv Cem Res 2014;26:101–13.

[24] British Standards BS EN 196-1. Methods of testing cement-Part 1: Determination of strength. 2005.

[25] Zsako J, Hints M. Use of thermal analysis in the study of sodium carbonate causticization by means of dolomitic lime. J Therm Anal Calorim 1998;53:323–31.

[26] Mun KJ, So SY, Soh YS. The effect of slaked lime, anhydrous gypsum and limestone powder on properties of blast furnace slag cement mortar and concrete. Constr Build Mater 2007;21:1576–82.

Figure Captions:

Figure 1 UCS development of reactive MgO and Na_2CO_3 activated GGBS pastes (a) 4% Na_2CO_3 + MgO_M; (b) 4% Na_2CO_3 + MgO_H; (c) 6% Na_2CO_3 + MgO_M; 8% Na_2CO_3 + MgO_M

Figure 2 Drying shrinkage of 4% Na_2CO_3 + MgO_H activated GGBS pastes

Figure 3 Drying shrinkage of GGBS pastes activated by Na_2CO_3 + MgO_M

Figure 4 XRD patterns of reactive MgO and Na_2CO_3 activated GGBS pastes at 28 d (a) two types of MgO with 4% Na_2CO_3; (b) MgO_M with 8% Na_2CO_3. Notations: C: C-S-H, CC: calcite, CN: sodium calcium carbonate, G: gehlenite hydrate, Ht: hydrotalcite-like phases, N: sodium carbonate.

Figure 5 TG/DTG curves of reactive MgO and Na_2CO_3 activated GGBS pastes at 28 d (a) and (b) TG and DTG of two types of MgO with 4% Na_2CO_3; (c) and (d) TG and DTG of MgO_M with 8% Na_2CO_3

Figure 6 Relationship between CBW and UCS of the pastes with different types and contents of MgOs and 4% of Na_2CO_3

Figure 7 SEM pictures of reactive MgO and Na_2CO_3 activated GGBS pastes at 3 d (a) N4, (b) N4H5, (c) N4M5, and (d) N8

Figure 8 SEM pictures of reactive MgO modified Na_2CO_3 activated GGBS pastes at 28 d (a) N4, (b) N4H5, (c) N4M5, and (d) N8

Table 1 Physico-chemical properties of the raw materials used in this study

Label		MgO_H	MgO_M	GGBS
Chemical composition (%)	MgO	97.5	93.2	8
	CaO	1	0.9	40
	Cl	0.2	-	-
	SiO_2	1	0.9	37
	Fe_2O_3	0.035	0.5	-
	Al_2O_3	-	0.22	13
	Mn	0.006	-	-
	Na_2O	-	-	0.3
	K_2O	-	-	0.6
	SO_3	0.85	-	2.5
Reactivity* (s)		10	100	-
Specific surface area (m^2/g)		110.82	9.005	0.493

*Measured according to the acetic acid test [16]

Table 2 Mix compositions with various sodium carbonate and reactive MgO contents (by weight of GGBS) and two types of reactive MgOs

Na_2CO_3 content /%	Paste notation	MgO_H content /%	MgO_M content /%
4	N4	-	-
	N4H5	5	-
	N4H7.5	7.5	-
	N4H10	10	-
	N4M5	-	5
	N4M7.5	-	7.5
	N4M10	-	10
6	N6	-	-
	N6M5	-	5
	N6M7.5	-	7.5
	N6M10	-	10
8	N8	-	-
	N8M5	-	5
	N8M7.5	-	7.5
	N8M10	-	10

Table 3 Weight losses in percentage calculated from TG/DTG curves

Paste denotation	Curing age					
	3 d			28 d		
	Δm_1 (<250 °C)	Δm_2 (250-450 °C)	Δm_t (40-800 °C)	Δm_1 (<250 °C)	Δm_2 (250-450 °C)	Δm_t (40-800 °C)
N4	2.79	3.42	8.33	3.85	1.85	8.94
N4M5	3.19	3.13	8.67	4.40	2.38	9.69
N4M10	3.24	4.73	10.60	5.06	2.73	10.67
N4H5	5.44	4.96	13.68	5.98	4.31	14.20
N4H10	5.96	5.88	15.84	7.47	5.68	17.08
N8	4.75	4.29	13.87	6.32	2.83	13.92
N8M5	5.04	4.69	14.22	6.61	3.45	14.71
N8M10	4.42	4.17	12.72	6.71	3.53	15.17

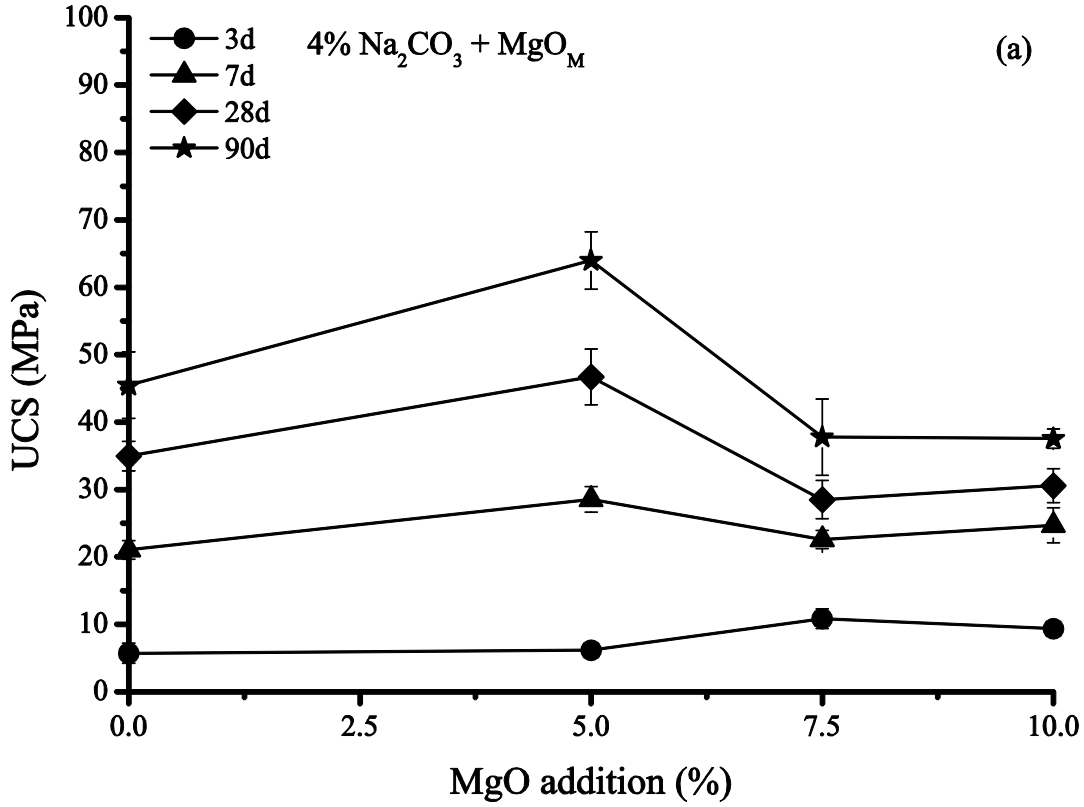
3d
7d
28d
90d
4% Na_2CO_3 + MgO_M
(a)
UCS (MPa)
MgO addition (%)
0
10
20
30
40
50
60
70
80
90
100
0.0
2.5
5.0
7.5
10.0

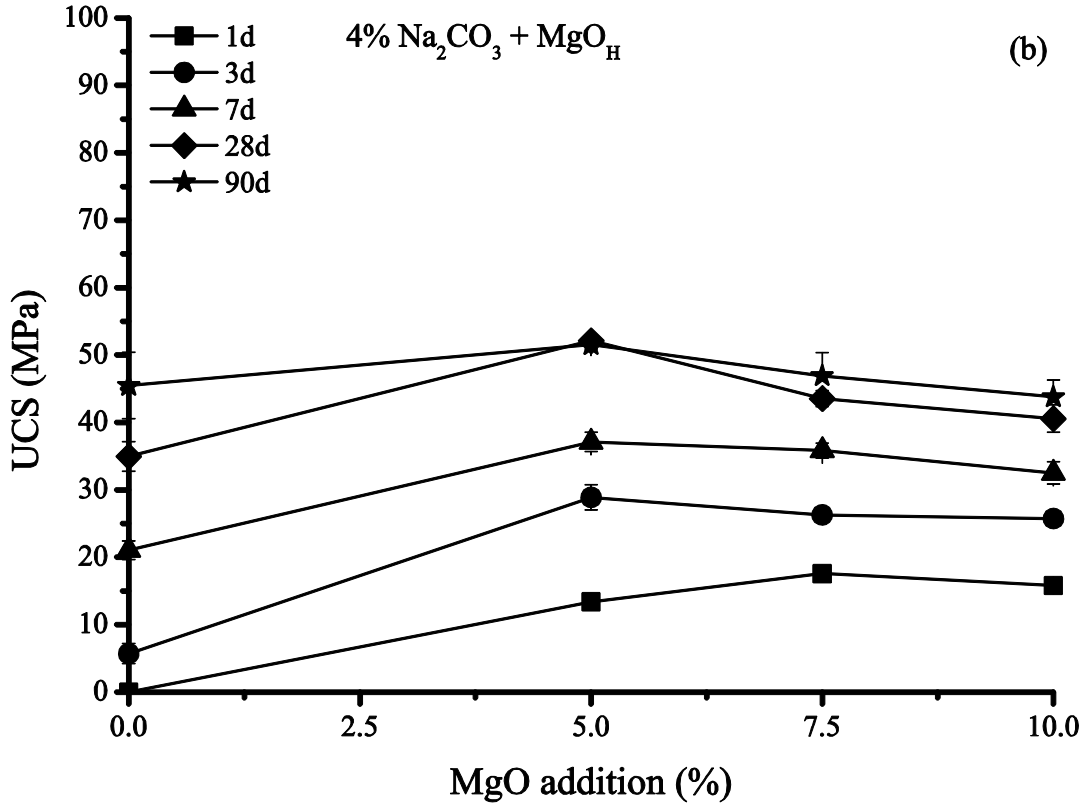
1d
3d
7d
28d
90d
4% Na_2CO_3 + MgO_H
(b)
UCS (MPa)
MgO addition (%)
0
10
20
30
40
50
60
70
80
90
100
0.0
2.5
5.0
7.5
10.0

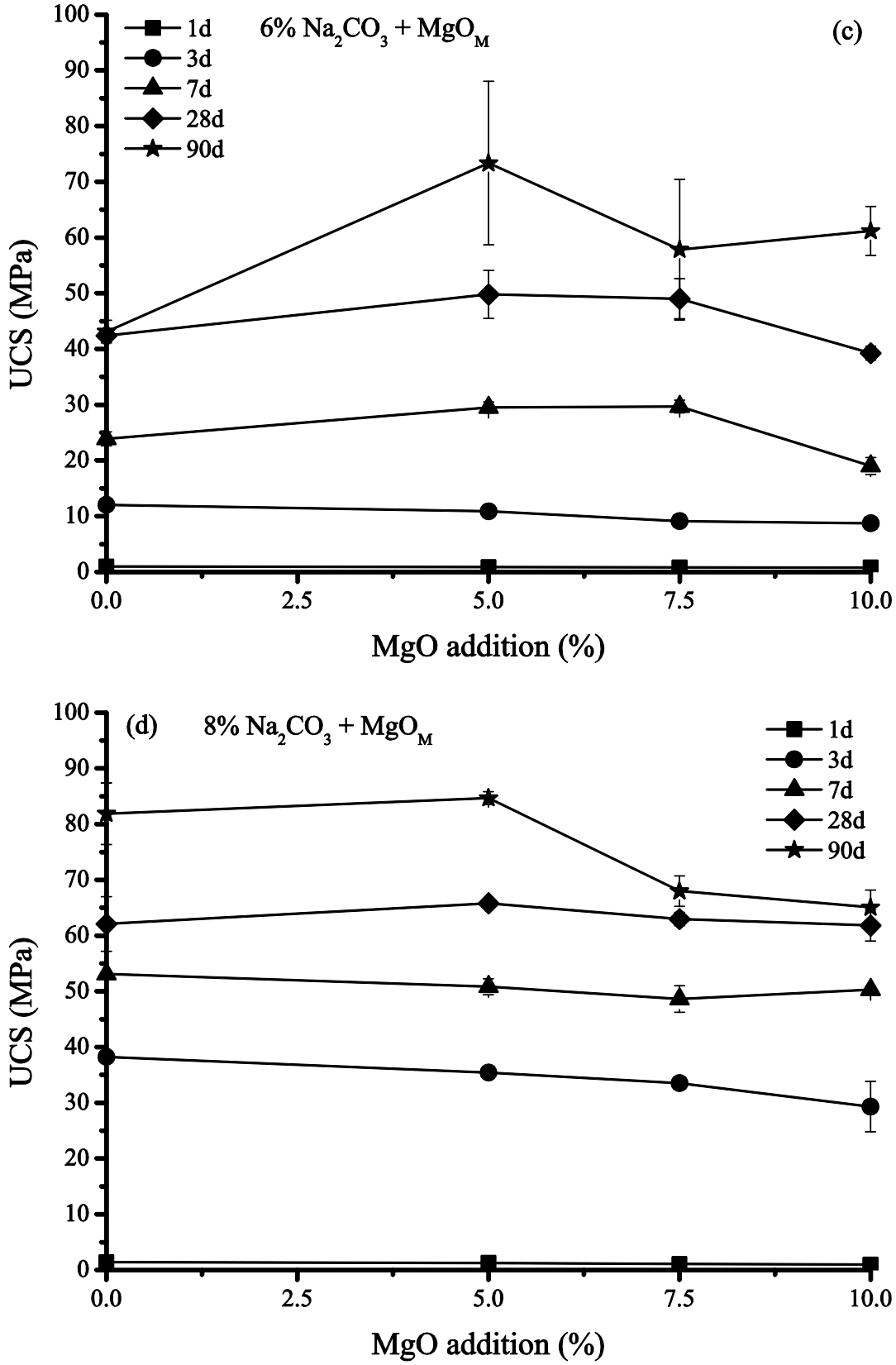
(c)
6% Na_2CO_3 + MgO_M
1d
3d
7d
28d
90d
UCS (MPa)
MgO addition (%)
(d)
8% Na_2CO_3 + MgO_M
1d
3d
7d
28d
90d
UCS (MPa)
MgO addition (%)

Fig. 1

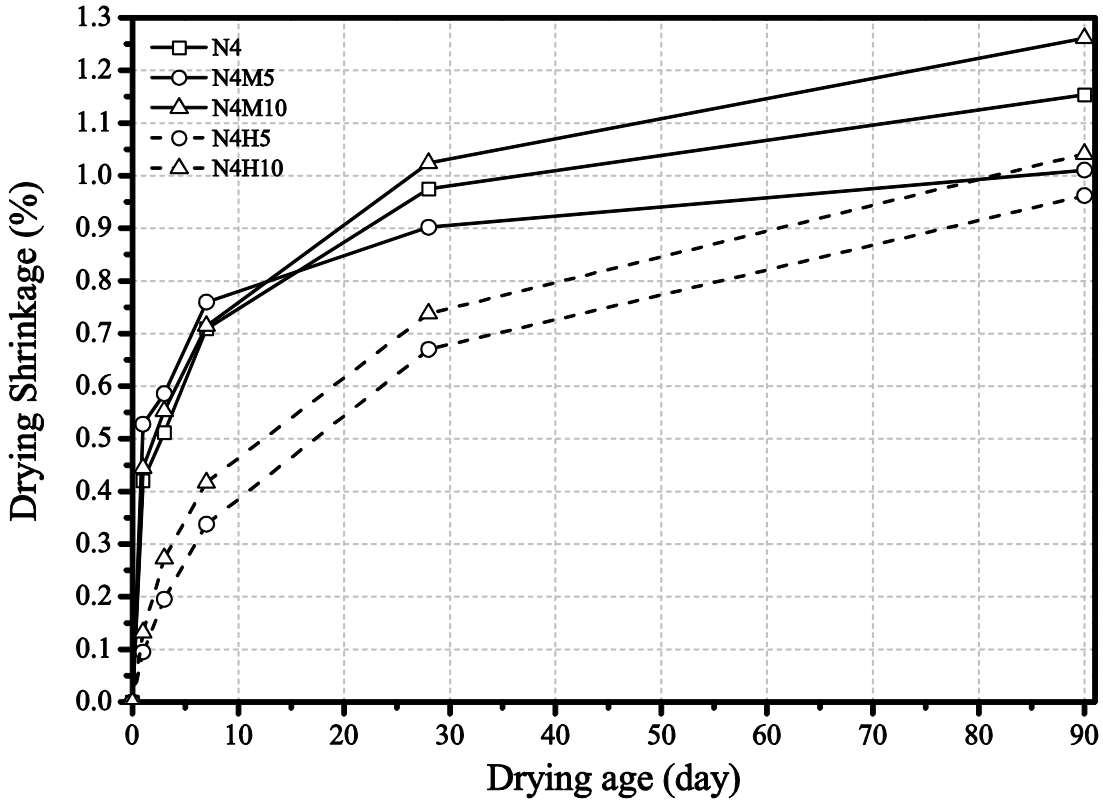
N4
N4M5
N4M10
N4H5
N4H10
Drying Shrinkage (%)
Drying age (day)
0.0
0.1
0.2
0.3
0.4
0.5
0.6
0.7
0.8
0.9
1.0
1.1
1.2
1.3
0
10
20
30
40
50
60
70
80
90

Fig. 2

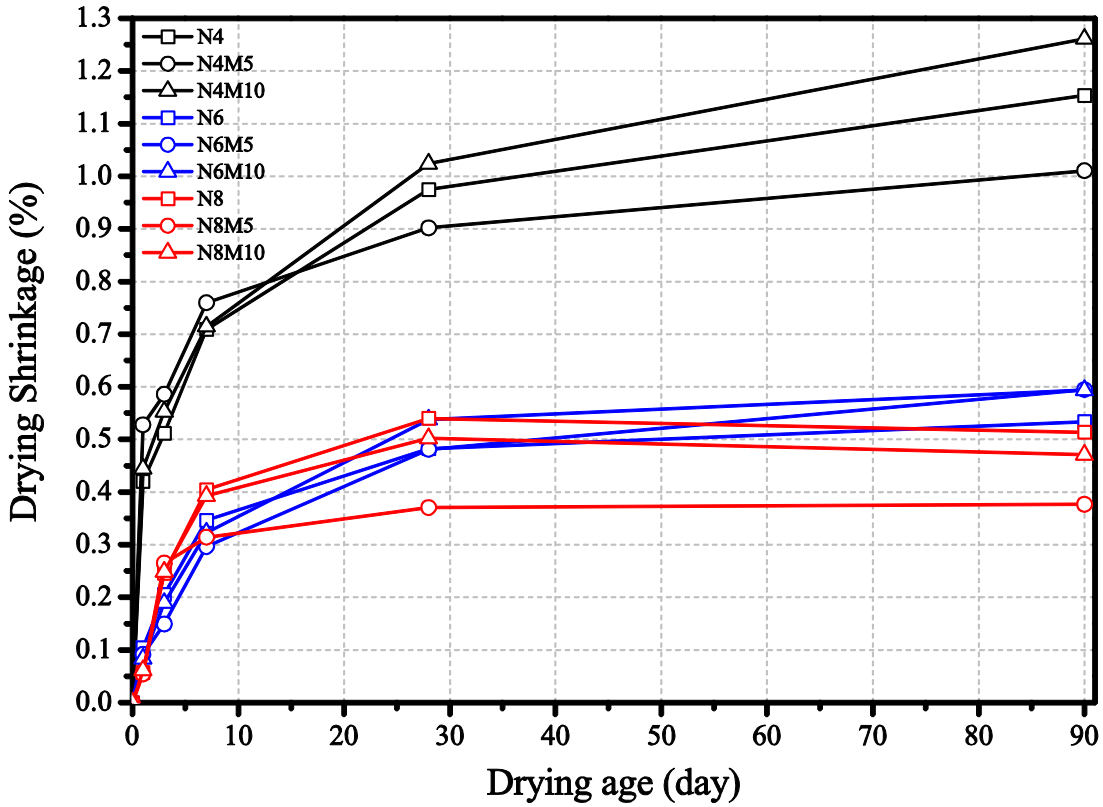
N4
N4M5
N4M10
N6
N6M5
N6M10
N8
N8M5
N8M10
Drying Shrinkage (%)
Drying age (day)
0.0
0.1
0.2
0.3
0.4
0.5
0.6
0.7
0.8
0.9
1.0
1.1
1.2
1.3
0
10
20
30
40
50
60
70
80
90

Fig.3

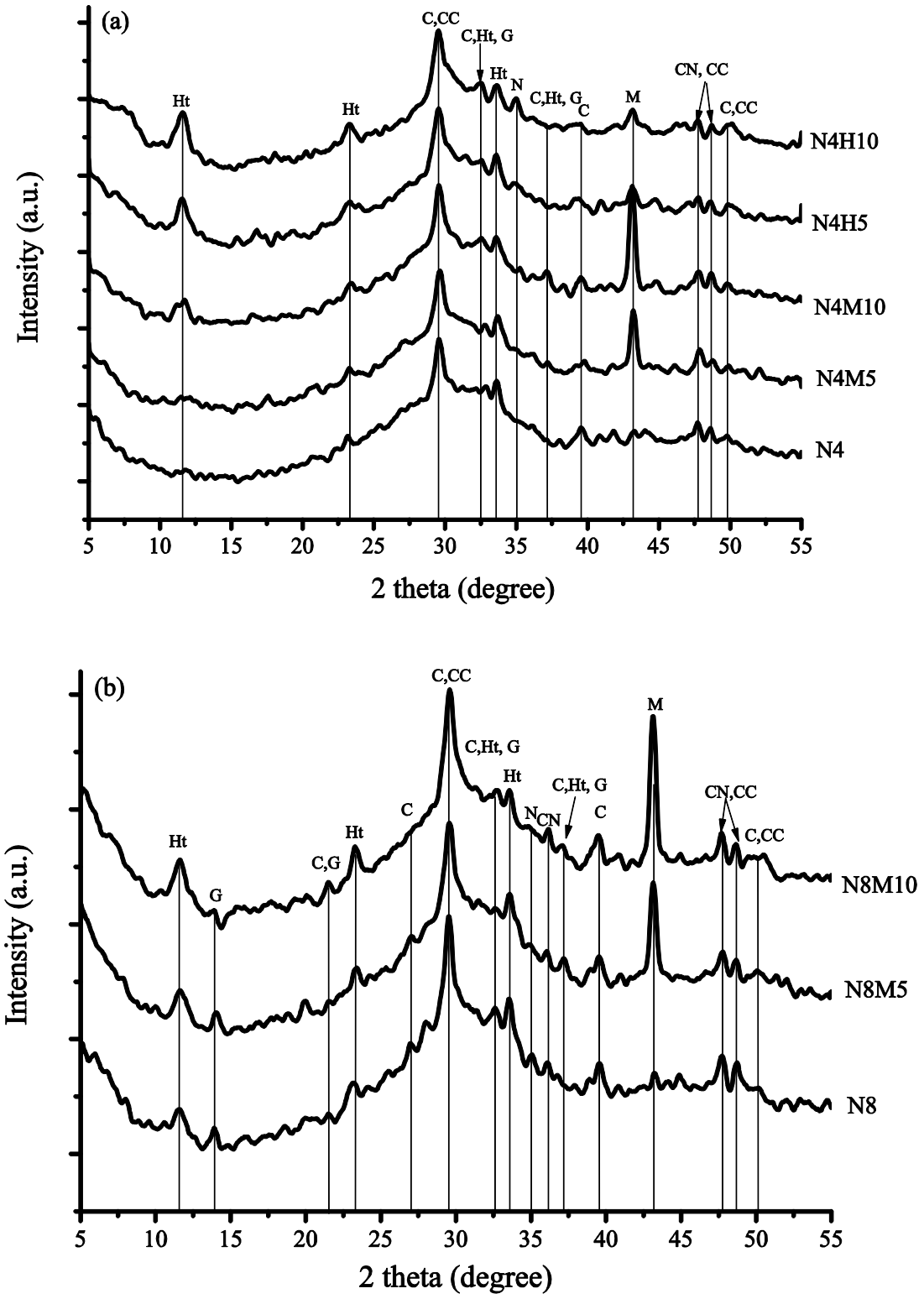
(a)
C,CC
C,Ht, G
Ht
N
C,Ht, G
C
M
CN, CC
C,CC
Ht
Ht
N4H10
N4H5
N4M10
N4M5
N4
Intensity (a.u.)
5
10
15
20
25
30
35
40
45
50
55
2 theta (degree)
(b)
C,CC
M
C,Ht, G
Ht
C,Ht, G
CN,CC
C
N
CN
C
C,CC
Ht
C,G
Ht
G
N8M10
N8M5
N8
Intensity (a.u.)
5
10
15
20
25
30
35
40
45
50
55
2 theta (degree)

Fig. 4

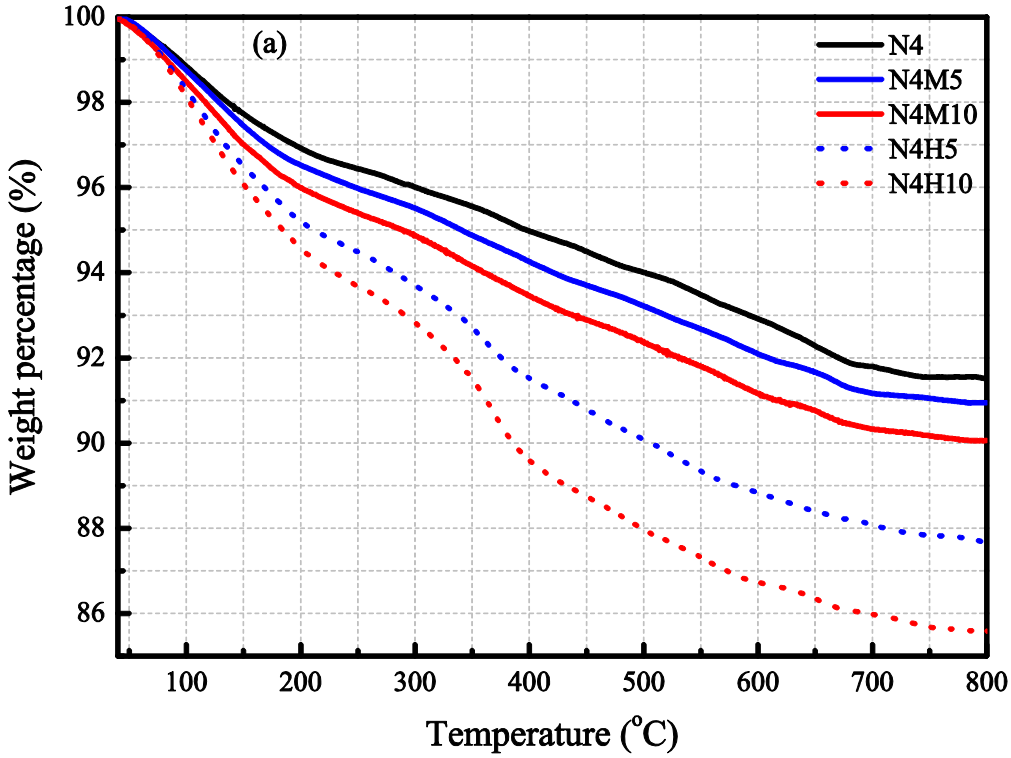
(a)
N4
N4M5
N4M10
N4H5
N4H10
Weight percentage (%)
Temperature (°C)
100
98
96
94
92
90
88
86
100
200
300
400
500
600
700
800

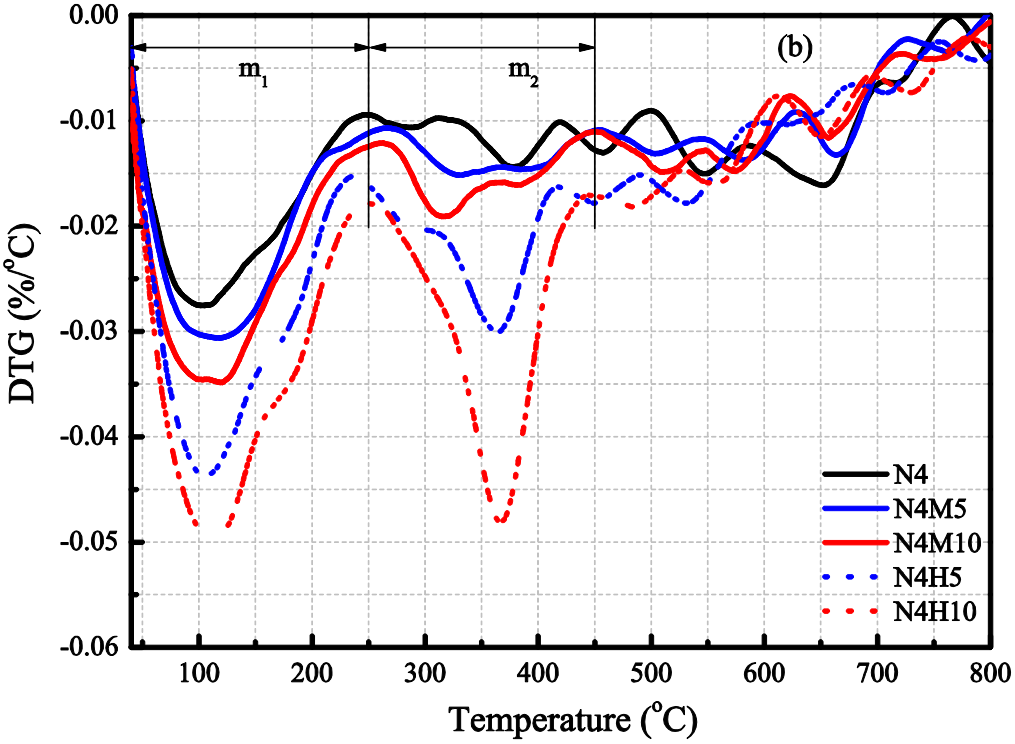
(b)
m1
m2
N4
N4M5
N4M10
N4H5
N4H10
DTG (%/°C)
Temperature (°C)
0.00
-0.01
-0.02
-0.03
-0.04
-0.05
-0.06
100
200
300
400
500
600
700
800

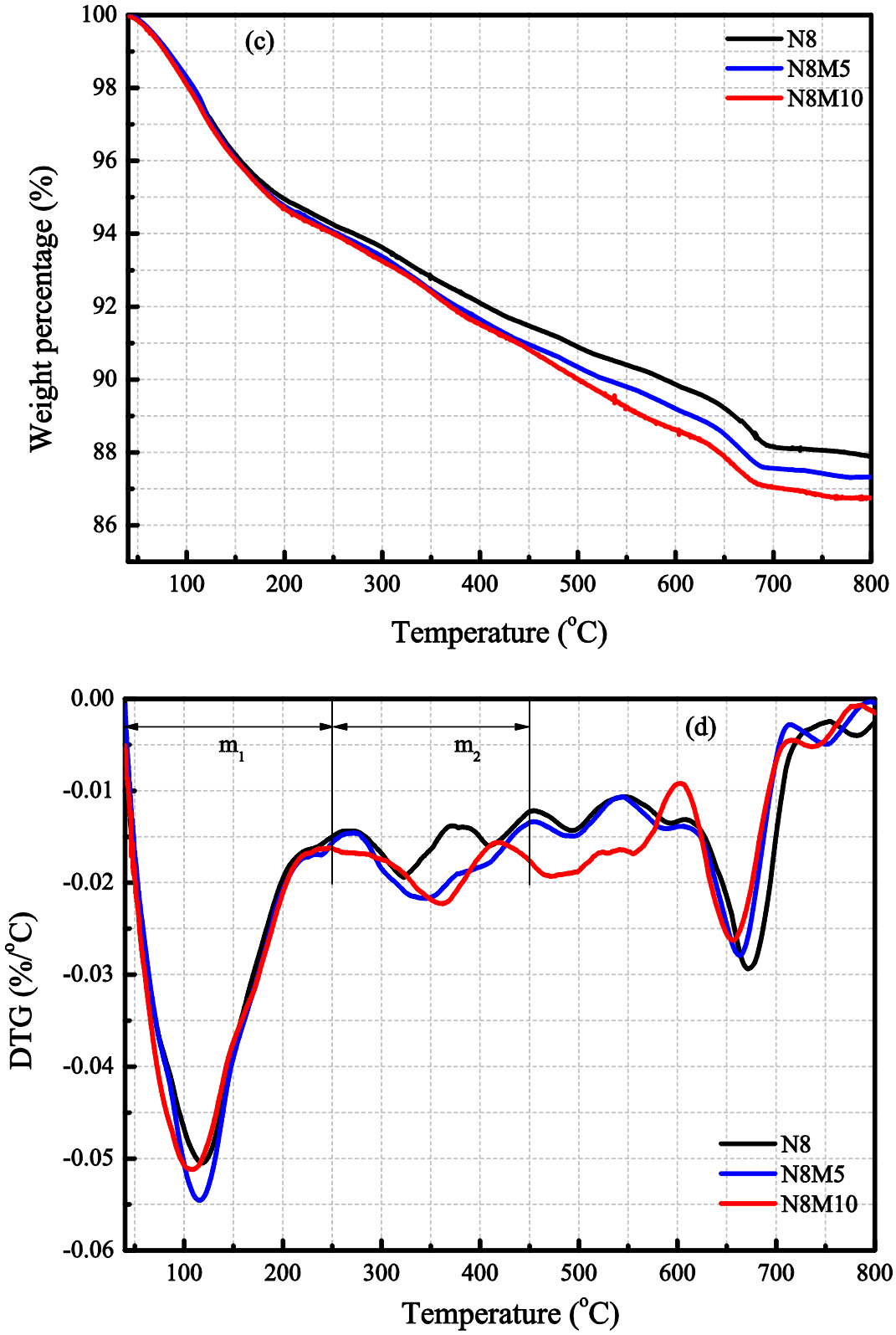
(c)
N8
N8M5
N8M10
Weight percentage (%)
Temperature (°C)
(d)
m1
m2
DTG (%/°C)
Temperature (°C)

Fig. 5

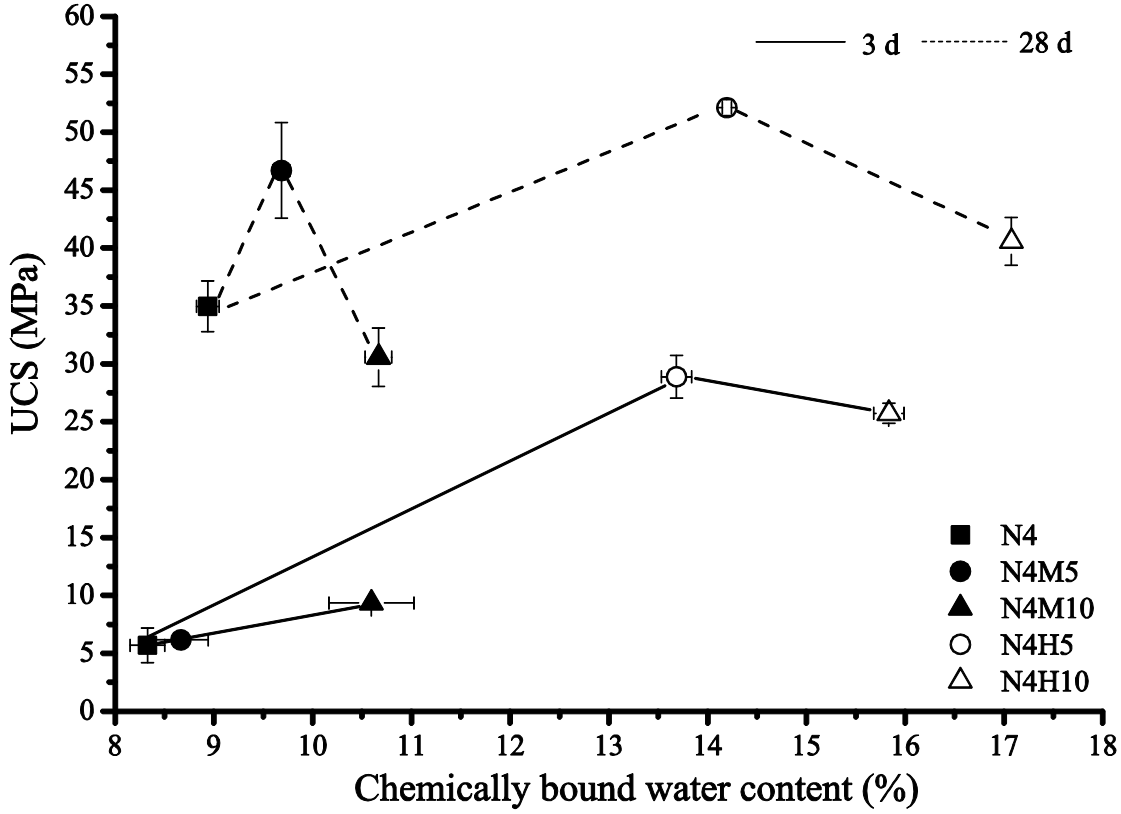
3 d
28 d
UCS (MPa)
Chemically bound water content (%)
N4
N4M5
N4M10
N4H5
N4H10
0
5
10
15
20
25
30
35
40
45
50
55
60
8
9
10
11
12
13
14
15
16
17
18

Fig. 6

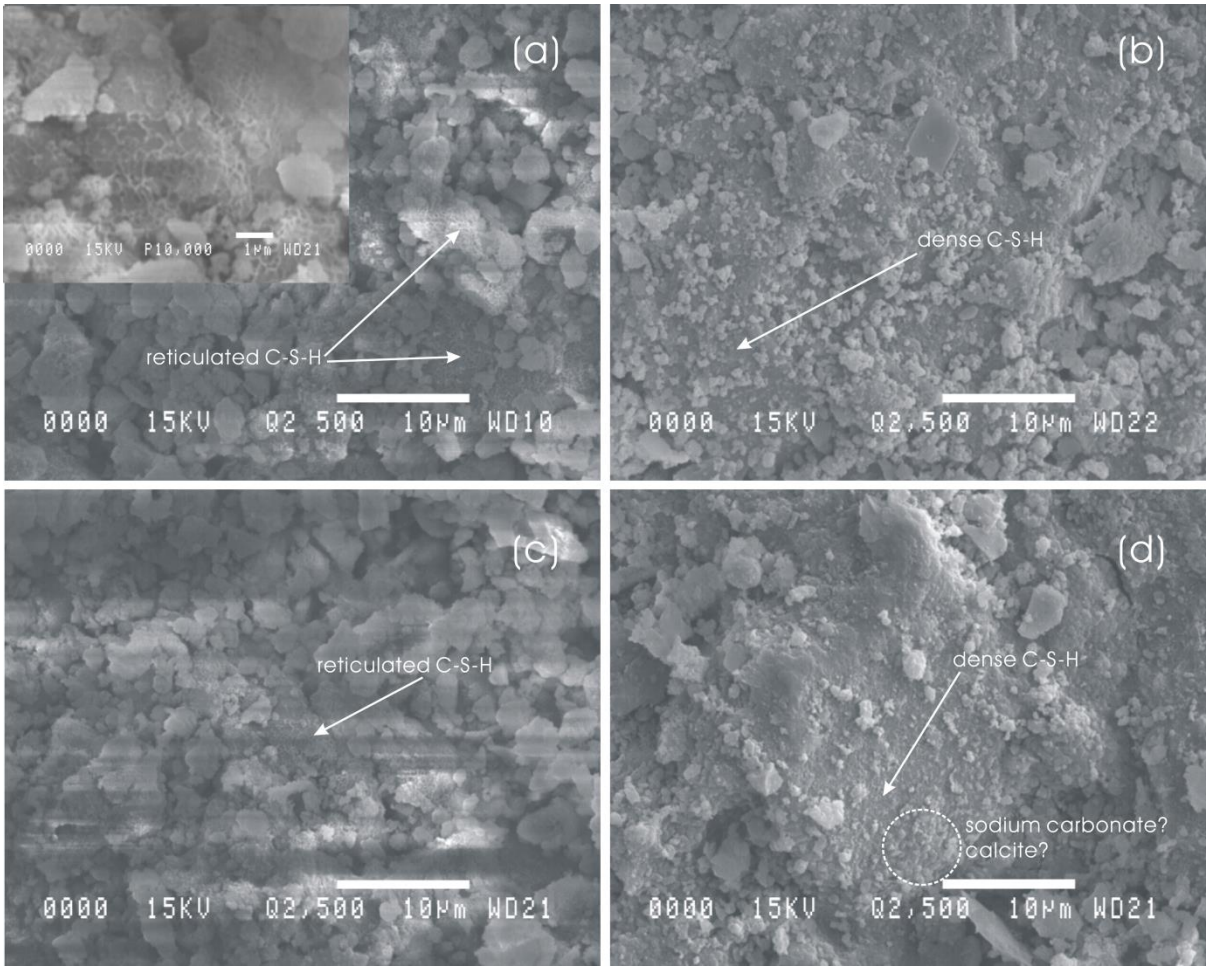
(a)
0000 15KV P10,000 1μm WD21
reticulated C-S-H
0000 15KV Q2 500 10μm WD10
(b)
dense C-S-H
0000 15KV Q2,500 10μm WD22
(c)
reticulated C-S-H
0000 15KV Q2,500 10μm WD21
(d)
dense C-S-H
sodium carbonate?
calcite?
0000 15KV Q2,500 10μm WD21

Fig. 7

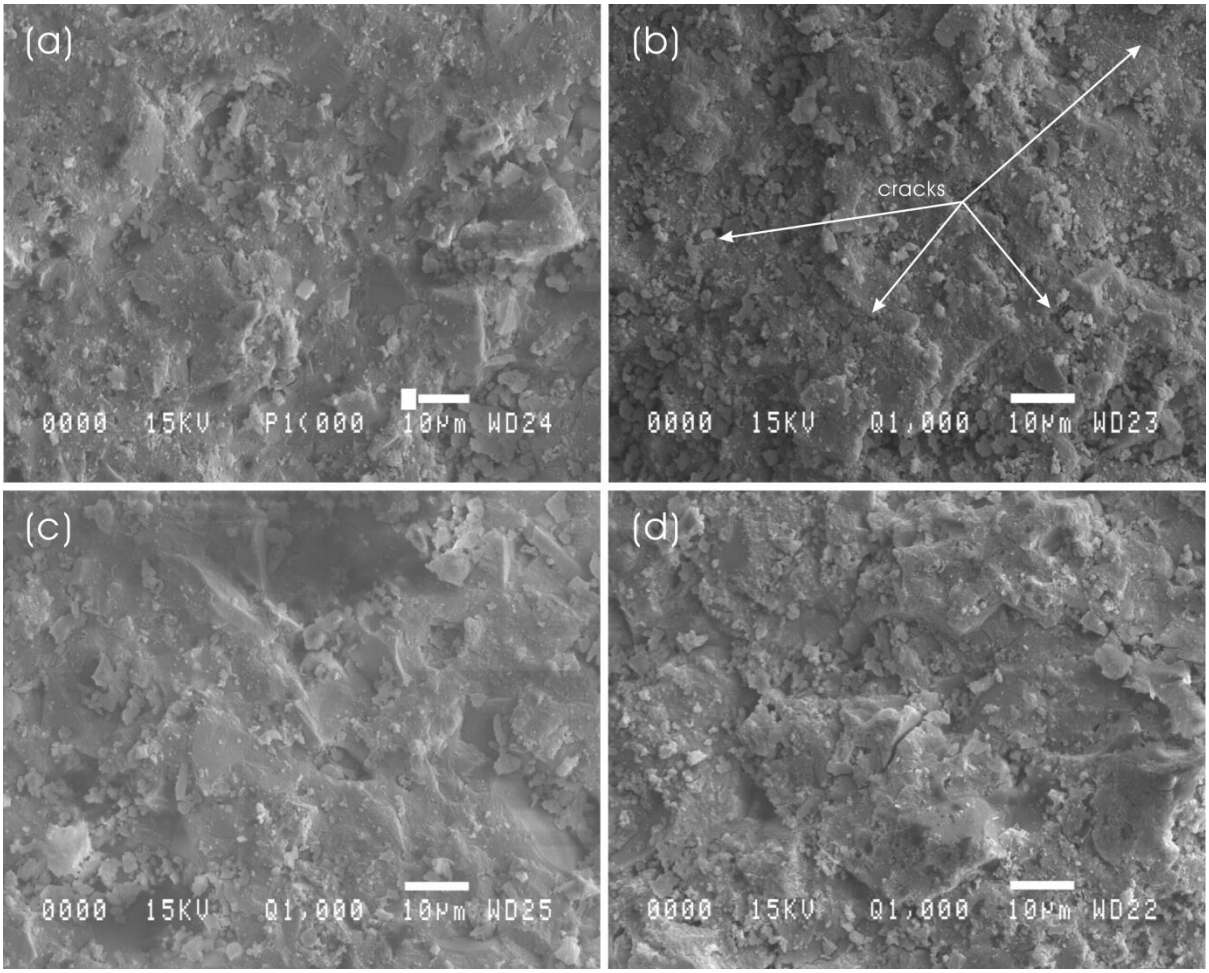
(a)
0000 15KV P1(000 10μm WD24
(b)
cracks
0000 15KV Q1,000 10μm WD23
(c)
0000 15KV Q1,000 10μm WD25
(d)
0000 15KV Q1,000 10μm WD22

Fig. 8